Cellular/Molecular

Endogenous Tumor Necrosis Factor α (TNFα) Requires TNF Receptor Type 2 to Generate Heat Hyperalgesia in a Mouse Cancer Model

Cristina E. Constantin,[1] Norbert Mair,[1] Claudia A. Sailer,[1] Manfred Andratsch,[1] Zhen-Zhong Xu,[3] Michael J. F. Blumer,[2] Nadja Scherbakov,[1] John B. Davis,[4] Horst Bluethmann,[5] Ru-Rong Ji,[3] and Michaela Kress[1]

[1]Division of Physiology, Department of Physiology and Medical Physics and [2]Division of Clinical and Functional Anatomy, Innsbruck Medical University, 6020 Innsbruck, Austria, [3]Pain Research Center, Department of Anesthesiology, Brigham and Women's Hospital, Harvard Medical School, Boston, Massachusetts 02115, [4]Discovery Technology Group, Research and Development, GlaxoSmithKline, Harlow, Essex CM19 5AW, United Kingdom, and [5]Roche Center for Medical Genomics, 4070 Basel, Switzerland

To provide a tool to investigate the mechanisms inducing and maintaining cancer-related pain and hyperalgesia, a soft tissue tumor/metastasis model was developed that is applicable in C57BL/6J wild-type and transgenic mice. We show that the experimental tumor-induced heat hyperalgesia and nociceptor sensitization were prevented by systemic treatment with the tumor necrosis factor α (TNFα) antagonist etanercept. In naive mice, exogenous TNFα evoked heat hyperalgesia *in vivo* and sensitized nociceptive nerve fibers to heat *in vitro*. TNFα enhanced the expression of the nociceptor-specific heat transducer ion channel transient receptor potential vanilloid 1 (TRPV1) and increased the amplitudes of capsaicin and heat-activated ionic currents via p38/MAP (mitogen-activated protein) kinase and PKC (protein kinase C). Deletion of the tumor necrosis factor receptor type 2 (TNFR2) gene attenuated heat hyperalgesia and prevented TRPV1 upregulation in tumor-bearing mice, whereas TNFR1 gene deletion played a minor role. We propose endogenous TNFα as a key player in cancer-related heat hyperalgesia and nociceptor sensitization that generates TRPV1 upregulation and sensitization via TNFR2.

Key words: **cancer-induced pain; heat hyperalgesia; primary afferent neurons; TNFα; TNF receptor type 2; TRPV1**

Introduction

Cancer is one of the leading causes of death, and in advanced stages 75–95% of the patients experience cancer-related pain, including a local hypersensitivity (hyperalgesia) to mechanical and/or thermal stimuli (Mantyh et al., 2002). The improvement of cancer pain therapies is impeded by our rudimental knowledge of the basic mechanisms and chemical mediators leading to cancer pain. In the past few years, mouse models of bone cancer-, skin cancer-, and neuropathic cancer-induced pain and hyperalgesia have been developed in C3H or BALB/c mice (Schwei et al., 1999; Honore et al., 2000; Wacnik et al., 2001; Shimoyama et al., 2002). Injection of fibrosarcoma cells into the femur of C3H mice resulted in development of a tumor mass accompanied by behavioral changes that closely resembled some aspects of human disease: animals showed signs of tenderness and ongoing and movement-evoked pain, which were well correlated with the tumor growth and the degree of bone destruction (Schwei et al., 1999; Honore et al., 2000). In the surroundings of the tumor, sprouting of epidermal nerve fibers was found, which was accompanied by an increase in excitability of "pain-sensing" neurons, so-called nociceptors (Cain et al., 2001a,b; Wacnik et al., 2001). Progression of tumor growth leads to a variety of local changes, such as the chemotaxis of immune cells (macrophages, leukocytes, and thrombocytes) and the production of mediators that are also found in inflamed tissue, e.g., cytokines (Alexander et al., 1998). Especially the proinflammatory and proalgesic cytokine tumor necrosis factor α (TNFα) may be of importance in this respect, because it is one of the first cytokines produced and released in the inflammatory cascade.

In the present study, we aimed to address the mechanisms of cancer pain and hyperalgesia and the contribution of TNFα. In the tumor tissue, cytokine protein concentrations were determined, and treatment with the soluble receptor etanercept was used to neutralize endogenous TNFα. To define the importance of specific TNF receptor subtypes or ion channels, mice carrying null mutations for the respective genes were investigated. We have therefore established a soft tissue tumor/metastasis model in the C57BL/6J mouse strain that allowed recording from nociceptive primary afferents under controlled *in vitro* conditions in transgenic and wild-type C57BL/6J mice. Correlative data from *in vivo*, *in vitro*, and biochemical assays suggest a contribution of tumor necrosis factor receptor type 2

Received Oct. 1, 2007; revised Feb. 27, 2008; accepted April 2, 2008.

This work was supported by Wilhelm Sanderstiftung Grant 1996.058.3 and Fonds zur Förderung der Wissenschaftlichen Forschung Grant P18444 (M.K.). We thank J. Partlic, M. Doblander, and S. S. Strasser for expert technical assistance and Dr. M. Reindl for helpful advice with macrophage staining.

Correspondence should be addressed to Prof. Michaela Kress, Division of Physiology, Department of Physiology and Medical Physics, Innsbruck Medical University, Fritz-Pregl-Strasse 3, A-6020 Innsbruck, Austria. E-mail: michaela.kress@i-med.ac.at.

DOI:10.1523/JNEUROSCI.4476-07.2008

 0270-6474/08/285072-10$15.00/0

(TNFR2) and a TNFα-dependent upregulation and sensitization of transient receptor potential vanilloid 1 (TRPV1).

Materials and Methods

Tumor cell culture and implantation. Lung carcinoma cells (ETCC clone 1642; European Collection of Cell Cultures, Wiltshire, UK) cultivated in DMEM (PAA, Vienna, Austria) with 4 mM L-glutamine and 10% fetal bovine serum were grown to confluence and passaged once a week. Tumor cells were prepared for implantation by pouring off the media and rinsing with PBS. Trypsin-EGTA (1×; Invitrogen, Paisley, UK) was added for 2 min to detach cells from the flask. The enzymatic reaction was stopped with 1 ml of DMEM. Just before implantation, cells were counted, washed twice, and then resuspended in PBS for implantation. Mice were anesthetized with isoflurane (Baxter, Vienna, Austria), and 7×10^5 lung carcinoma cells in 25 μl of PBS were injected subcutaneously in the plantar and dorsal side of the mouse hindpaw.

Drug preparation and administration. Twenty mice received the TNFα antagonist etanercept (Enbrel; 1 mg/d; Wyeth, Taplow, Maidenhead, UK) by systemic intraperitoneal injection starting from the day of tumor cell inoculation over the whole period of investigation. Mouse TNFα 5 μg/ml (Roche Diagnostics, Basel, Switzerland) was aliquoted (50 ng/10 μl) and kept at −20°C. Subsequent dilutions before administrations were made in PBS for treatment of mice, which received TNFα intraplantarly (10 ng/10 μl). In electrophysiological recordings, TNFα was applied for 10 min to the receptive fields of primary afferents or for 1 min to single neurons in culture.

Tumor size and cytokine quantification. At the terminal day (7–10 d after carcinoma cell inoculation), the footpad diameter of the injected (ipsilateral) and noninjected (contralateral) paw was determined using a caliper. The mice were killed by CO_2 inhalation, and plantar and dorsal tumors were dissected from the surrounding tissues and weighed.

Tumor and control tissue (spinal cord and muscle) were collected, homogenized in liquid nitrogen, and resuspended in ice-cold PBS containing 0.025% Tween 20 and protease inhibitor mixture (Sigma-Aldrich, St. Louis, MO). Tissue suspension was centrifuged at 16,000 × *g* for 20 min, and the protein content of both pellet and supernatant was determined using the Bradford assay. Tumor cells in culture were harvested and treated in the same way. Cytokine levels were determined using a 3-Bioplex mouse cytokine assay (IL1β, IL6, and TNFα) from Bio-Rad (Hercules, CA) according to the manufacturer's protocol.

Tissue preparation for light and transmission electron microscopy. Mice were killed by ventilation with 100% CO_2, and the hindpaws with tumor were dissected and sectioned transversely. The tissue was fixed in 4% paraformaldehyde (PFA) in PBS (0.1 M), decalcified in 3% ascorbic acid in sodium chloride (0.15 M), dehydrated, and embedded in paraffin. Serial sections (5 μm) were made on an HM 355S microtome (Microm, Walldorf, Germany) and stained with hematoxylin–eosin. Other hindpaws with tumor were fixed in 2.5% glutaraldehyde, 2% paraformaldehyde buffered in sodium cacodylate (0.1 M), pH 7.4, and postfixed in 0.5% osmium tetroxide, 1% potassium hexacyanoferrate III in distilled water. Samples were decalcified as described above, followed by dehydration and embedment in Spurr's epoxy resin. Semithin sections (2 μm) were cut on a Reichert Ultracut S microtome (Leica Microsystems, Wetzlar, Germany) with a histo-jumbo-diamond knife (Diatome, Biel, Switzerland) (Blumer et al., 2002) and stained with toluidine blue. Ultrathin sections (80 nm) were cut on the same microtome with an ultra-diamond knife, mounted on dioxan-formvar-coated copper slot grids and stained with an aqueous solution of uranyl acetate (1%) and lead citrate. Ultrathin sections were examined with an electron microscope 10A (Zeiss, Oberkochen, Germany).

Semithin resin and histological paraffin sections were examined with a Zeiss Axioplan 2 and photographed as color images using Zeiss AxioCam HR and AxioVision 4.1. software.

Nerve fiber staining within the tumor. Tumor tissue was frozen on liquid nitrogen and cut on a cryostat (Microm). The respective sections were fixed for 20 min in 4% PFA, blocked in PBS containing 0.2% Triton X-100, 2% BSA, and 2% normal goat serum (NGS) for 120 min and incubated for 18 h with an anti-CGRP antibody (1:2000; Immunostar, Hudson, WI). Thereafter, sections were washed with PBS, incubated with a secondary antibody (1:4000; Alexa 594 goat anti-rabbit; Invitrogen), and examined on a Zeiss Axioplan 2 microscope equipped with a Zeiss Axioscan CCD 24 bit color digital camera.

Macrophage staining within the tumor. Fixed sections were permeabilized in PBS containing 0.1% Triton X-100 (PBS-T) for 20 min. After blocking the endogenous peroxidase with 0.3% H_2O_2 in PBS, nonspecific binding sites were blocked with 9% NGS and 3% BSA in PBS-T. Tumor sections were incubated with an anti-cd11b antibody (0.1 μg/ml; BD Biosciences, San Jose, CA) overnight, followed by detection with the avidin–biotin complex (Vectastain ABC Elite Kit). Immunoreaction products were visualized by addition of 0.06% 3.3′-diaminobenzidine and 0.003% H_2O_2. Sections were counterstained with hematoxylin and processed as described above.

Quantitative PCR: TaqMan real-time PCR analysis. For analysis of mRNA levels, total RNA was isolated from murine lumbar dorsal root ganglion (DRG) neurons of untreated and treated animals immediately after preparation by using TRI reagent (Sigma-Aldrich) according to the manufacturer's instructions. Reverse transcription to cDNA was performed using the GeneAmp RNA PCR Kit (Applied Biosystems, Foster City, CA). Each cDNA sample was analyzed for expression of TRPV1, TNFR1, and TNFR2 by real-time quantitative PCR using the TaqMan 5′ nuclease assays Mm01246301_m1 (TRPV1), Mm01182929_m1 (TNFR1), Mm00441889_m1 (TNFR2), and Mm99999915_g1 [glyceraldehyde-3-phosphate dehydrogenase (GAPDH)]. The reactions were performed in a MicroAmp Fast Optical 96-Well Reaction Plate (Applied Biosystems) using the 7500 Fast Real-Time PCR System (Applied Biosystems) for thermal cycling and real-time fluorescence measurements. The PCR cycle protocol consists of 10 min at 95°C and 40 two-step cycles of 15 s each at 95°C and of 1 min at 60°C. Positive and negative controls were included in all the experiments, and each sample was run in triplicate for each PCR. Threshold cycle (C_T) values were recorded as a measure of initial template concentration. Relative fold changes in RNA levels were calculated by the $\Delta\Delta C_T$ method using GAPDH as a reference standard. C_T values from triplicate samples were averaged and then subtracted from the reference standard, yielding ΔC_T. The mean of the ΔC_T values with SDs of the treated animals was set in relation to the control (nontreated) animals.

Western blot analysis. Lumbar DRGs (L3–L5) from mice with and without tumor were homogenized in lysis buffer (10 mM Tris-HCl, pH 7.4, protease inhibitor mixture from Sigma-Aldrich) using a glass potter. Crude membranes were obtained by centrifugation (20 min at 100,000 × *g*) and resuspension of the respective pellet in 20 mM Tris-HCl, pH 7.4. Protein samples were separated by SDS-PAGE and transferred to polyvinylidene difluoride membranes. These membranes were probed with anti-TRPV1 antibody (0.4 μg/ml) or anti-α-tubulin antibody (0.4 μg/ml; Sigma-Aldrich). Antibody-stained bands were visualized by incubation with HRP-conjugated secondary antibodies (Santa Cruz Biotechnology, Santa Cruz, CA) followed by enhanced chemiluminescence reagent (GE Healthcare, Little Chalfont, UK). Immunoreactive bands were quantified by densitometric scanning using TotalLab software (Nonlinear Dynamics, Newcastle upon Tyne, UK).

Behavioral studies. A total number of 205 C57BL/6J mice of either sex (>6 weeks of age) and three different genotypes (TNFR1$^{-/-}$, TNFR2$^{-/-}$, and TRPV1$^{-/-}$) were used in all experiments. The generation of homozygous TNFR1-deficient (TNFR1$^{-/-}$), TNFR2-deficient (TNFR2$^{-/-}$), and TRPV1-deficient (TRPV1$^{-/-}$) mice by gene targeting has been described previously (Rothe et al., 1993; Erickson et al., 1994; Davis et al., 2000). The background strain of TNFR1$^{-/-}$, TNFR2$^{-/-}$, and TRPV1$^{-/-}$ mice is C57BL/6J. All animal experiments were approved by the Austrian Ethical Commission. Mice were housed on a 12 h light/dark cycle with *ad libitum* access to mouse chow and water. Standard testing procedures were used to quantify signs of pain-like behavior. The area tested was the plantar side of the hindpaw, where the tumor cells were inoculated. Mechanical sensitivity at the tumor site was determined with calibrated von Frey monofilaments with bending forces between 2.8 and 45.3 mN. The withdrawal threshold was determined by increasing and decreasing stimulus intensity on the basis of the up–down method (Sommer and Schafers, 1998). Heat sensitivity was assessed using the Hargreaves test (Hargreaves et al., 1988). Paw-withdrawal latency in re-

sponse to an increasing heat stimulus was measured automatically (Ugo Basile, Comerio, Italy).

Skin-nerve preparation and single-fiber recordings. An *in vitro* skin-nerve preparation was used to investigate the properties of the afferent nerve fibers innervating the skin of the mouse dorsal hindpaw as described previously (Kress et al., 1992; Koltzenburg et al., 1997). Briefly, the preparation was superfused (15 ml/min) with an oxygen-saturated modified synthetic interstitial fluid solution containing (in mM) 108 NaCl, 3.48 KCl, 3.5 $MgSO_4$, 26 $NaHCO_3$, 1.7 NaH_2PO_4, 2.0 $CaCl_2$, 9.6 sodium gluconate, 5.5 glucose, and 7.6 sucrose at a temperature of 31 ± 1°C and pH 7.4 ± 0.05. Action potentials of single sensory neurons were recorded extracellularly from fine filaments dissected from the saphenous nerve, amplified (5000-fold), filtered (low-pass 1 kHz, high-pass 100 Hz), visualized on oscilloscope, and stored on a PC-type computer with the Spike/Spidi software package (Forster and Handwerker,1990). The fibers were characterized as unmyelinated (C) according to their conduction velocity. The receptive field was identified by mechanical probing of the skin with a glass rod; standard heat stimuli linearly raising the intracutaneous temperature from 31 ± 1°C to 47°C were applied. A fiber was considered heat sensitive if three or more action potentials were evoked during the stimulus. The heat threshold was defined as the temperature that elicited the third spike of the response. In tumor-injected mice, electrophysiological recordings were performed 7–10 d after inoculation, when a tumor mass had formed at the injection site.

DRG cell culture. Lumbar DRGs were harvested, treated enzymatically, and dissociated as described previously (Obreja et al., 2002, 2005). The resulting cell suspension was washed, plated on coverslips coated with poly-L-lysine/laminin, cultivated in synthetic serum-free medium (supplemented TNB; Biochrom, Vienna, Austria) at 37°C in 5% CO_2 and used within 32 h.

Quantitative analysis of TRPV1 immunoreactivity. After 2 d in culture, DRG neurons were stimulated with TNFα (10 ng/ml) for 1 or 2 h. The cultures were fixed with 4% PFA for 30 min and immunostained with TRPV1 (1:1000; anti-rabbit; Millipore Bioscience Research Reagents, Temecula, CA). The intensity of staining was measured with NIH Image J. Four cultures were included for each group.

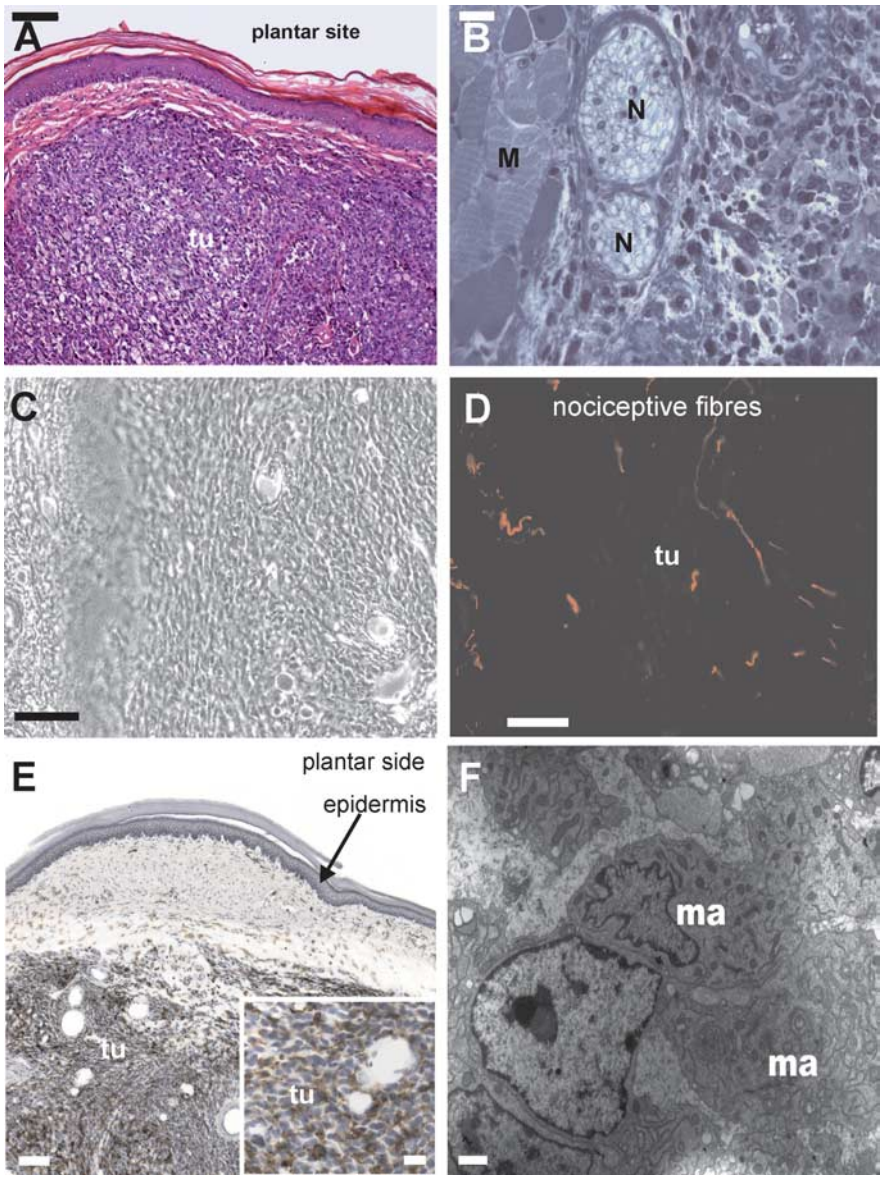

Figure 1. Tumor histology. ***A***, Hematoxylin–eosin (HE) staining of paraffin-embedded longitudinal sections through the mouse hindpaw 10 d after carcinoma cell inoculation (plantar side overview). The tumor tissue (tu) was located below the dermis. Scale bar, 100 μm. ***B***, Toluidine blue staining of resin-embedded cross sections through the mouse hindpaw. Tumor tissue was distributed through the whole hindpaw surrounding nerve fibers (N) and muscles (M). Scale bar, 20 μm. ***C***, ***D***, Innervation of tumor tissue by sensory afferent fibers. ***C***, Phase-contrast image showing an overview of the tumor mass. ***D***, Labeling of unmyelinated primary afferent fibers with anti-CGRP antibody revealed that sensory neurons sprout into the tumor tissue. Scale bars: ***C***, ***D***, 100 μm. ***E***, Tumor tissue contained tumor and immune cells. Macrophage labeling with biotin-conjugated anti CD11 (brown) revealed that these immune cells were spread throughout the whole tumor mass. Scale bar, 100 μm; inset, 25 μm. ***F***, Electron microscopy images showing a macrophage (ma) in the vicinity of tumor cell. Scale bar, 1 μm.

Patch-clamp recordings. Using the voltage-clamp configuration of the patch-clamp technique, whole-cell ion currents were recorded from isolated neurons as previously described (Obreja et al., 2002, 2005). External solution contained the following (in mM): 145 NaCl, 5 KCl, 2 $CaCl_2$, and 1 $MgCl_2$ (all Sigma-Aldrich) and 10 glucose and 10 HEPES (Merck, Darmstadt, Germany), at pH 7.3 adjusted with NaOH (Merck). Patch-clamp pipettes from borosilicate glass (Science Products, Hofheim, Germany), filled with internal solution [(in mM) 148 KCl, 2 $MgCl_2$, 2 Na_2-ATP, 0.1 $CaCl_2$, and 1 EGTA (all from Sigma-Aldrich) and 10 HEPES (Merck), at pH 7.3 adjusted with KOH (Merck)], had a resistance of 2–4 MΩ. Currents were filtered at 2.9 kHz, sampled at 3 kHz, and recorded using an EPC 9 (HEKA, Lambrecht/Pfalz, Germany) and the Pulse v8.74 software (HEKA). A seven-barrel system with common outlet was used for fast drug administration and heat stimulation (Dittert et al., 1998). Heat-activated inward currents (I_{heat}) were elicited at −80 mV holding potential by applying ramp-shaped heat stimuli at 60 s intervals (linear temperature increase from room temperature to 50°C within 5 s). TNFα (1 ng/ml) was used as intermittent conditioning stimulus (60 s) followed by a 3 min washout. In some experiments TNFα was applied together with p38 mitogen-activated protein (MAP) kinase inhibitor SB203580 (EMD Biosciences, San Diego, CA) or protein kinase C (PKC) inhibitor BIM1 (EMD Biosciences). Capsaicin was purchased from Sigma-Aldrich.

Statistical analysis. For detailed statistical analysis, the SigmaStat 3 program was used. Data are presented as mean ± SEM and were analyzed using one-way repeated-measures ANOVA for comparison between groups and test days, followed by a Student's *t* test if not otherwise stated. Differences were considered statistically significant at $p < 0.05$.

Results

Tumor-induced heat and mechanical hyperalgesia

Subcutaneous inoculation of lung carcinoma cells into the plantar and dorsal side of the mouse hindpaw led to development of a tumor mass, which grew continuously with time (Fig. 1). At the terminal day (7–10 d after carcinoma cell inoculation), the diameter of the ipsilateral paw was increased 2.7-fold compared with the contralateral side ($n = 11$). The mean size of the plantar tumor was 25.77 ± 4.78 mg, whereas the dorsal tumor had a mean weight of 17.39 ± 0.47 mg. Tumor tissue contained densely packed cells at all mitotic stages and surrounded muscular structures, nerve bundles, and blood vessels but did not invade the tarsal bones (Fig. 1*A*,*B*). Similar to other cancer pain models, carcinoma cell inoculation induced mechanical hyperalgesia. Paw-withdrawal thresholds in response to mechanical von Frey stimulation decreased from 41.21 ± 2.20 mN before to 13.37 ± 2.59 mN (ANOVA, with Fisher's *post hoc* test, $p < 0.001$) on day 10 after inoculation (supplemental Fig. 1*A*, available at www.jneurosci.org as supplemental material).

At the same time, tumor growth led to an increasing heat hyperalgesia: in the Hargreaves test, paw-withdrawal latencies decreased significantly from 7.33 ± 0.25 s before to 5.82 ± 0.41 s on the second day (ANOVA, $p < 0.001$) and reached latencies as low as 4.09 ± 0.47 s on day 10 after carcinoma cell inoculation (Fig. 2*A*). Labeling with a specific anti-CGRP antibody revealed that the tumor was densely innervated by peptidergic unmyelinated fibers (Fig. 1*C*,*D*). The skin in the vicinity of the tumor is easily accessible, and therefore, our newly developed soft tissue cancer/metastasis model offers the unique advantage of allowing one to directly record discharge activity from peripheral afferents associated with the tumor tissue under *in vitro* conditions. In general, the subpopulations of unmyelinated primary afferents innervating the skin attached to the tumor area were similar to those found in healthy skin (Table 1). However, 31% (17 of 54) of the C-fibers investigated in the tumor-treated mice exhibited irregular resting activity compared with only 7% in healthy skin. The rate of ongoing activity in fibers from tumor mice ranged from 0.2 to 1.5 impulses (imp)/s with a mean rate of 0.46 ± 0.09 imp/s. Ten of the spontaneously active fibers had an irregular pattern of discharge, two discharged regularly at a rate of 1–2 Hz, and five exhibited burst-like discharges at intervals ranging from 13.2 to 59.4 s. Among the spontaneously active fibers, two were classified as mechanosensitive, three were heat sensitive, and six reacted to both mechanical and heat stimuli. The remaining six fibers were not further classified. In the skin from the control (naive) mice, 7% (4 of 54) of the C-fibers exhibited resting activity ranging from 0.1 to 0.83 imp/s (mean, 0.49 ± 0.17 imp/s).

No difference in the proportions of mechanosensitive (61% in both groups) or heat-sensitive fibers between the tumor and the control group (70% vs 65%) was observed. However, the mean discharge rates during heat responses in the tumor group were significantly higher than controls (4.18 ± 0.58 imp/s vs 2.79 ± 0.53 imp/s; $p < 0.001$, ANOVA) (Fig. 2*B*). In addition, the mean activation threshold temperatures of heat-sensitive fibers were significantly lower in the tumor group than in controls [34.51 ± 0.51°C ($n = 38$) vs 37.30 ± 0.64°C ($n = 35$); $p < 0.001$, *t* test] (Fig. 2*C*). The majority of neurons in the tumor group (63%) were excited by very small rises in ambient temperature (<3°C) compared with 34% in healthy skin ($p < 0.02$, χ^2 test) (Fig. 2*C*). All observed changes point toward an increased heat sensitivity of nociceptors projecting into the tumor area as a functional correlate for the heat hyperalgesia observed *in vivo*. Immunocytochemistry with specific marker antibodies showed that the tumor tissue was densely infiltrated with macrophages (Fig. 1*E*,*F*), which are generally accepted as a major source of proinflammatory cytokines.

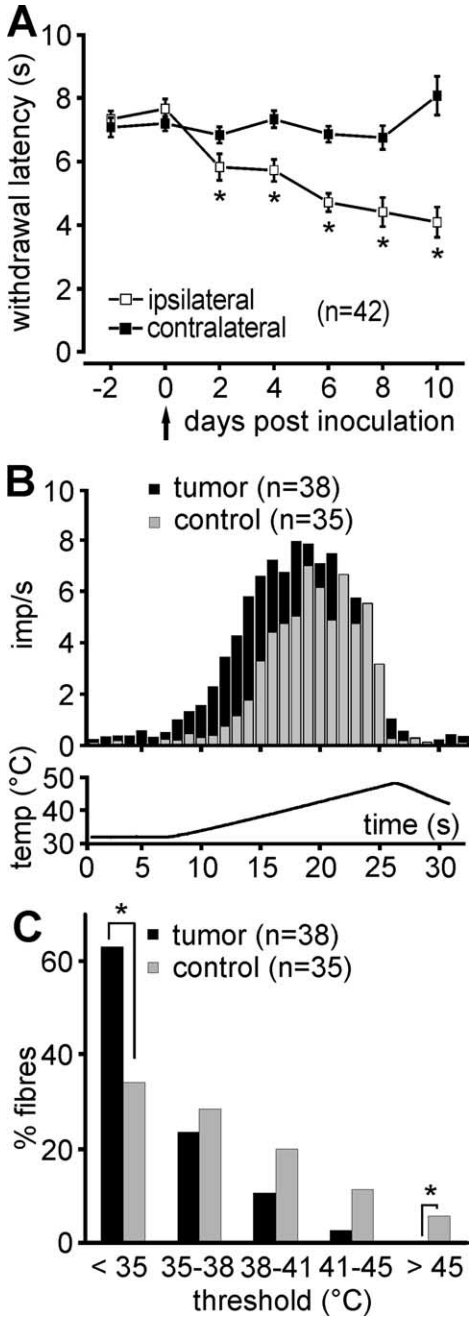

Figure 2. Tumor-induced heat hyperalgesia. ***A***, Paw-withdrawal latency (in seconds) in response to ramp-shaped heat stimuli applied to the plantar side of the hindpaw ipsilateral (□) and contralateral (■) to tumor cell inoculation ($n = 42$). After tumor induction, paw-withdrawal latency to heat stimuli applied to the tumor area (ipsilateral paw) decreased significantly ($p < 0.001$, ANOVA) starting from day 2 after injection and persisted over the 10 d of investigation. Asterisks indicate the values significantly different ($p < 0.05$) between ipsilateral and contralateral paw. ***B***, ***C***, Properties of heat-sensitive C-fibers innervating the dorsal site of the hindpaw recorded *in vitro*. ***B***, Discharge profiles of the heat-activated C-fibers. Mean discharge rates were significantly higher in heat-sensitive C-fibers from tumor mice ($n = 38$) than from control mice ($n = 35$; $p < 0.001$, ANOVA). ***C***, Distribution of the activation threshold temperatures of heat-sensitive C-fibers in tumor (black columns; $n = 38$) and healthy control (gray columns; $n = 35$) mice. Asterisks mark significant differences ($p < 0.05$, χ^2 test). temp, Temperature.

Endogenous TNFα and TNFR2 are required for tumor-induced heat hyperalgesia

We therefore searched for the presence of cytokines in the supernatant of tumor cells in culture and in tumor homogenates using a Bioplex ELISA assay. In cell culture supernatant or cell lysates, TNFα, IL1β, and IL6 concentrations were below the detection limits of the assay, suggesting that tumor cells *in vitro* do not release appreciable amounts of these cytokines. However, in tumor sample homogenates collected from mice that had received an injection of carcinoma cells, TNFα and IL1β were detected in pathophysiologically relevant concentrations (20.82 ± 0.22 pg/mg protein and 36.38 ± 12.72 pg/mg protein, respectively) whereas IL6 levels were considerably lower (1.43 ± 0.22 pg/mg protein) (Fig. 3*A*). Together, these data suggest that the increased heat sensitivity of polymodal nociceptors in the tumor area might be secondary to the release of cytokines (e.g., TNFα) from the tumor tissue, which in turn may induce nociceptor sensitization. We therefore investigated whether TNFα contributes to tumor-induced heat hyperalgesia and nociceptor heat sensitization. Daily systemic treatment with the TNFα-neutralizing soluble receptor etanercept (1 mg, i.p.) largely prevented the development of heat hyperalgesia in the tumor-bearing mice. Paw-withdrawal latencies in response to heat stimuli were very similar to those of healthy controls even 6 d after tumor induction (Fig. 3*B*). This beneficial effect was not attributable to treatment-induced reduction of tumor size, because the weight of the tumor mass was similar in tumor mice and tumor mice treated with etanercept [21.95 ± 3.39 mg ($n = 46$) vs 19.94 ± 3.44 mg ($n = 30$)]. A lower dose of etanercept (100 μg, i.p., daily) did not block initiation and maintenance of heat hyperalgesia after tumor development (supplemental Fig. 2*A*, available at www.jneurosci.org as supplemental material).

When etanercept treatment (1 mg/d) was started on day 7 after tumor cell inoculation, the paw-withdrawal latencies before and after treatment did not differ significantly (4.43 ± 0.23 s on day 6 vs 5.50 ± 0.52 s and 4.62 ± 0.86 s on days 8 and 10, respectively; $p > 0.05$, *t* test; $n = 8$) (supplemental Fig. 2*B*, available at www.jneurosci.org as supplemental material). This suggests that etanercept treatment is inefficient once heat hyperalgesia has developed. Furthermore, a beneficial effect on the tumor-induced mechanical hyperalgesia was observed neither with etanercept treatment nor in any of the knock-out mouse strains investigated (data not shown).

In vitro, the heat-sensitive fibers from tumor mice that had received 1 mg of etanercept daily showed significantly reduced heat responses compared with the nontreated tumor group (mean, 2.47 ± 0.44 after etanercept vs 4.18 ± 0.58 imp/s; $p < 0.001$, ANOVA) (Fig. 3*C*). In etanercept-treated mice, the mean heat response magnitudes were similar to those in the healthy control group (mean, 2.47 ± 0.44 vs 2.79 ± 0.53 imp/s; $p > 0.05$; ANOVA). We also found that the proportion of heat-sensitive fibers and the activation threshold temperatures of heat-sensitive fibers were not affected by the etanercept treatment (mean, 35.72 ± 0.90 vs 34.51 ± 0.51°C) (Fig. 3*D*). Thus, the neutralization of TNFα has a significant beneficial effect on cancer-induced heat hyperalgesia, and this suggests that TNFα is required for the development of nociceptor heat sensitization in our cancer pain model.

TNFα binds to two different types of receptors: TNFR1 and TNFR2. To delineate which of the two TNFα receptors was involved in the generation of heat hyperalgesia in the cancer pain model, behavioral experiments in mice with a deletion of either the TNFR1 ($TNFR1^{-/-}$) or TNFR2 ($TNFR2^{-/-}$) gene were performed. $TNFR1^{-/-}$ mice injected with tumor cells still showed significant (from day 6) heat hyperalgesia (Fig. 3*E*). Because these mice showed a smaller increase in paw diameter than did wild-type mice (0.35 ± 0.01 vs 0.48 ± 0.05 cm; $p < 0.05$, Mann–Whitney), this minor effect might be attributable to a reduced degree of inflammation rather than tumor growth. In mice with a deletion of the TNFR2 gene, no heat hyperalgesia developed until the very late stages of tumor development (Fig. 3*F*), suggesting that TNFR2 plays the predominant role in the generation of tumor-induced heat hyperalgesia.

Table 1. Fiber properties

Properties	Tumor	Tumor + etanercept	Control
Mechanical sensitivity	8	14	17
Mechanical sensitivity + spontaneous activity	2	3	1
Heat sensitivity	12	10	19
Heat sensitivity + spontaneous activity	3	0	1
Mechanical sensitivity + heat sensitivity	17	11	13
Mechanical + heat sensitivity + spontaneous activity	6	1	2
Only spontaneous activity	6	1	0
Total	54	40	53

Properties of primary afferent neurons innervating the dorsal side of the hindpaw recorded in an *in vitro* skin-nerve preparation from tumor mice, tumor mice treated with etanercept, and control (naive, uninjected) mice. Data are the number of fibers with each property.

TNFα-induced heat hyperalgesia and heat sensitization of sensory neurons

To investigate whether TNFα itself can induce heat hyperalgesia, the cytokine was administered by intraplantar injection in naive (control) mice. Within 30 min, TNFα (10 ng in 10 μl of PBS) induced a significant drop in paw-withdrawal latency in response to heat stimuli from 7.25 ± 0.51 s before to 3.41 ± 0.28 s at the injection site ($p < 0.001$, ANOVA; $n = 12$), which recovered to preinjection values within 24 h (Fig. 4*A*). Intraplantar injection of 10 μl of vehicle (PBS) did not induce any overt changes in paw-withdrawal latency at any of the time points tested (7.67 ± 0.4 s before vs 7.15 ± 0.68 s 30 min after injection; $p > 0.05$, ANOVA; $n = 6$). In the *in vitro* skin-nerve preparation, application of TNFα (1 ng/ml) to the receptive field induced a significant increase in heat response magnitudes in 42% (5 of 12) of heat-sensitive C-fibers obtained from healthy mice (mean, 1.62 ± 0.39 vs 3.25 ± 0.67 imp/s; $p < 0.001$, paired *t* test) (Fig. 4*B*). This sensitization occurred within 10 min after TNFα application. In addition, TNFα evoked ongoing activity in three of eight C-fibers and increased the rate of discharge in two of four fibers that initially exhibited resting activity. Together, the results indicate that TNFα has a direct effect on heat-sensitive nociceptors.

TNFα-induced sensitization of capsaicin and heat-activated currents

To address the cellular mechanism of the TNFα-induced nociceptor heat sensitization, patch-clamp recordings were performed in small-diameter DRG neurons using the whole-cell voltage-clamp configuration of the patch-clamp technique. Neurons responded to the TRPV1-selective agonist capsaicin (0.5 μM) with a slowly activating inward current (I_{cap}), which was significantly increased after a 60 s pretreatment with TNFα ($n = 13$; $p < 0.05$, Wilcoxon test) (Fig. 5*A*,*D*). Similarly, heat-activated inward currents (I_{heat}) were significantly increased after a conditioning stimulation with TNFα ($n = 21$; $p < 0.05$, Wil-

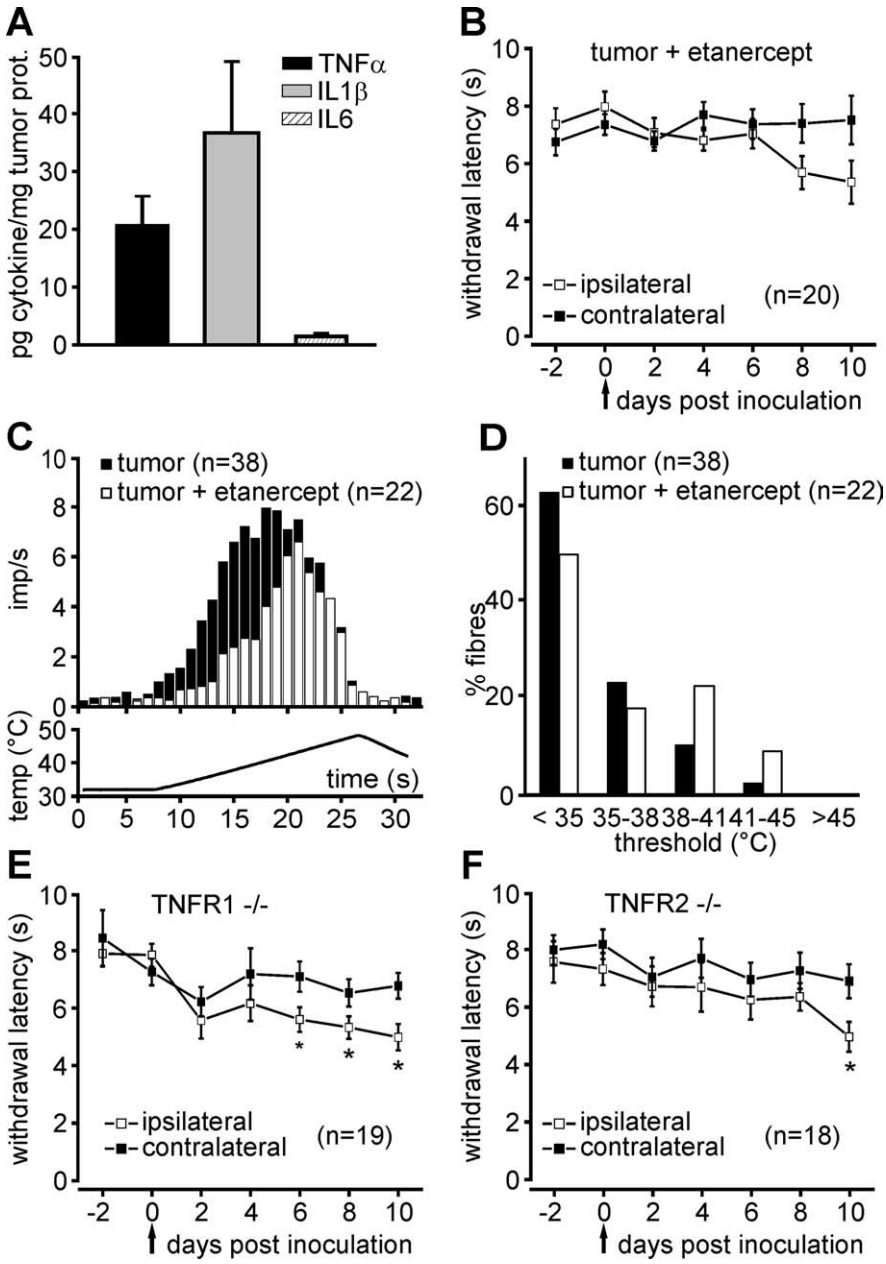

Figure 3. Tumor-induced heat hyperalgesia depended on TNFα and TNFR2. ***A***, Proinflammatory cytokines are produced at the tumor site. TNFα, IL1β, and IL6 levels (in picograms of cytokine per milligram of tumor protein) in tumor homogenates (plantar and dorsal) isolated from 11 mice. Cytokine levels of control tissues (muscle and spinal cord) were below detection limits of the assay (<0.3 pg/mg tissue protein). ***B***, The TNFα receptor body etanercept prevented tumor-induced heat hyperalgesia. Paw-withdrawal latency (in seconds) in response to ramp-shaped heat stimuli applied to the plantar side of the hindpaw ipsilateral (□) and contralateral (■) to tumor cell inoculation in tumor mice daily treated with etanercept ($n = 20$). Etanercept administered systemically abolished heat hypersensitivity in mice with tumor. ***C***, Discharge profiles of the heat-activated C-fibers. Mean discharge rates in response to heat stimulation were significantly lower in nociceptors obtained from tumor mice treated with etanercept ($n = 22$) than in those from tumor mice without treatment ($n = 38$; $p < 0.001$, ANOVA). ***D***, Distribution of the activation threshold temperatures of heat-sensitive C-fibers from nontreated tumor (black columns; $n = 38$) versus etanercept-treated tumor mice (white columns; $n = 22$). ***E***, Deletion of the TNFR1 gene delayed the onset of heat hyperalgesia in mice with tumor ($n = 19$). ***F***, Mice lacking the TNFR2 gene develop heat hyperalgesia only on day 10 after tumor induction ($n = 18$). Asterisks indicate the data points at which a significant difference between the ipsilateral and contralateral side was observed ($p < 0.05$, ANOVA). prot., Protein; temp, temperature.

coxon test) (Fig. 5*B*,*E*). Moreover, TNFα induced a shift in the activation threshold temperature of I_{heat} from 43° before to 41°C after TNFα ($p < 0.05$, Wilcoxon test) (Fig. 5*C*). The p38 MAP kinase inhibitor SB203580 (1 μM) and the PKC inhibitor BIM1 (1 μM) completely abolished the potentiating effect of TNFα on both the capsaicin- and heat-activated currents (Fig. 5*D*,*E*). Moreover, TNFα induced decrease in heat activation threshold was abolished both by the p38/MAPK inhibitor SB203580 (1 μM; 42.93 ± 0.64°C before vs 42.51 ± 0.45°C after TNFα stimulation; $p > 0.05$, Wilcoxon test) or the PKC inhibitor BIM1 (1 μM; 42.08 ± 0.59°C before vs 41.38 ± 0.69°C after TNFα stimulation; $p > 0.05$, Wilcoxon test). Together, these data suggest that TNFα sensitizes the heat transducer ion channel TRPV1 neurons via a p38 MAP kinase/PKC-dependent pathway in sensory neurons.

TNFα-mediated regulation of TRPV1 protein expression

Since its cloning, the nociceptor-specific capsaicin-sensitive ion channel TRPV1 has evolved as a multimodal transducer of nociceptive stimuli (Caterina et al., 1997; Tominaga et al., 1998). It is essential for the development of heat hyperalgesia in inflammatory pain models (Davis et al., 2000; Chuang et al., 2001). Therefore, we investigated whether there were differences in TRPV1 expression between control and tumor-bearing mice. Ten days after tumor cell inoculation, the amount of TRPV1 protein was 2.2-fold increased in L3, L4, and L5 DRGs from wild-type mice with tumor ($n = 6$) compared with healthy (control) mice (Fig. 6*A*,*B*). In mice with a deletion of TNFR2 gene, TRPV1 protein levels were not significantly different in healthy compared with tumor conditions (Fig. 6*B*), suggesting that TNFα induces upregulation of TRPV1 via this receptor subtype in the tumor-bearing mice. Consistent with these results, TNFα (10 ng/ml) stimulation of cultured DRG neurons for 1 and 2 h increased the TRPV1 immunostaining and protein levels (Fig. 6*C*,*D*). Further evidence for the involvement of TRPV1 in tumor-induced heat hyperalgesia was obtained from mice lacking the TRPV1 gene. In TRPV1$^{-/-}$ mice, inoculation of tumor cells did not induce heat hyperalgesia (Fig. 6*E*). In quantitative mRNA analysis using Taqman PCR, however, no significant difference in TRPV1 mRNA expression levels was found between tumor and control mice (data not shown). These data are consistent with previous reports on posttranscriptional upregulation of TRPV1 in an inflammatory pain model (Ji et al., 2002), and they support the hypothesis that heat hyperalgesia requires the expression of TRPV1 (Davis et al., 2000; Chuang et al., 2001).

Discussion

In the present study, we established a soft tissue cancer/metastasis model in mice to investigate the mechanisms leading to tumor-induced pain. We found that (1) there was tumor growth with sprouting of peptidergic nerve fibers into the tumor mass; (2) this was accompanied by progressive mechanical and heat hyperalgesia and a significant nociceptor sensitization; (3) TNFα activating TNFR2 was a key player in the development of cancer-related heat hyperalgesia; (4) TNFα caused heat hyperalgesia *in vivo* and augmented nociceptor heat sensitivity *in vitro*; (5) TNFα sensitized TRPV1 channels via p38/MAP kinase- and PKC-dependent pathways and upregulated TRPV1 in cultured DRG neurons; (6) tumor-induced heat hyperalgesia was associated with an upregulation of TRPV1 protein content at the posttranscriptional level, which was abolished in TNFR2$^{-/-}$ mice; and (7) TRPV1 was required for tumor-induced hyperalgesia *in vivo*.

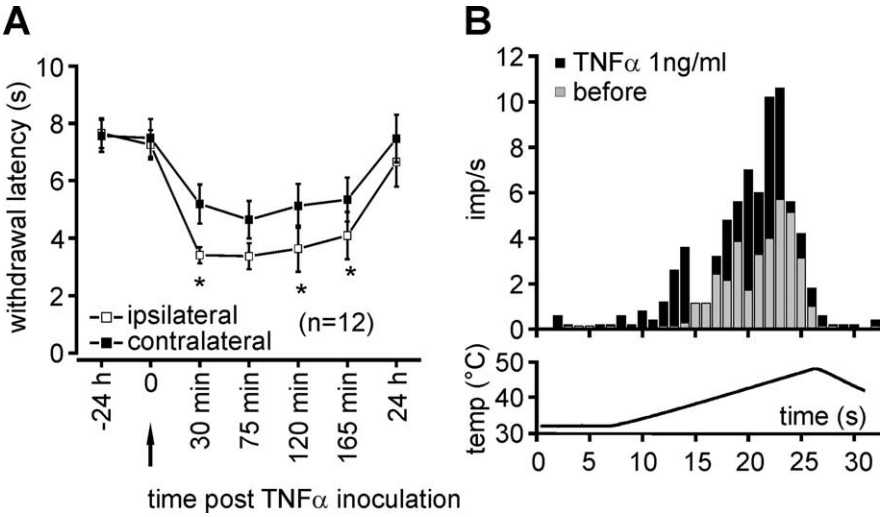

Figure 4. TNFα induced heat hyperalgesia in control (naive) mice. ***A***, Intraplantar injection of TNFα 10 ng/10 μl evoked a drop of paw-withdrawal latency in response to heat stimulation. Asterisks indicate the data points at which a significant difference ($p < 0.05$, ANOVA, with Student–Newman–Keuls *post hoc* test) between the ipsilateral (□) and contralateral (■) sides was observed. ***B***, Discharge profiles of heat-sensitive C-fibers before and after TNFα (1 ng/ml) application on their receptive fields in an *in vitro* skin-nerve preparation. TNFα application for 10 min induced a significant increase in the mean rate of discharge of the heat C-nociceptors investigated ($p < 0.001$, ANOVA; $n = 5$). temp, Temperature.

Recently, several animal models were developed to study bone (Schwei et al., 1999; Wacnik et al., 2001), skin (Sasamura et al., 2002), and neuropathic cancer pain (Shimoyama et al., 2002). Among these, the bone cancer model in C3H mice was most extensively used to study the contribution of particular proalgesic mediators in tumor-induced pain. Injection of fibrosarcoma cells into the mouse femur or calcaneus bone led to cancer-associated pain with bone destruction by osteoclasts (Schwei et al., 1999) and severe mechanical hypersensitivity of the respective limb (Wacnik et al., 2005). TNFα is generally accepted as a potent activator of osteoclasts, and subcutaneous injection of TNFα induced mechanical hyperalgesia (Wacnik et al., 2005) and mechanical sensitization of C-nociceptors (Junger and Sorkin, 2000). Therefore, it is not surprising that the TNFα antagonist etanercept reduced mechanical hypersensitivity in the bone cancer model (Wacnik et al., 2005). Thus, the bone cancer model has provided some insight into cancer-related mechanical hyperalgesia. However, very few studies have addressed cancer-induced heat hyperalgesia so far: in a melanoma model, tumor development was accompanied by signs of ongoing pain and heat hyperalgesia (Sasamura et al., 2002), and in the bone cancer model, a recent study has reported upregulation of TRPV1 in distinct subpopulations of DRG neurons (Niiyama et al., 2007). In the same model, disruption of the TRPV1 gene or administration of a TRPV1 antagonist attenuated both ongoing and movement-evoked nocifensive behaviors, which were suggested to occur as a consequence of tissue acidosis after bone cancer induction (Ghilardi et al., 2005). None of these studies, however, has addressed the occurrence and mechanisms of heat hyperalgesia associated with cancer/metastasis. For the first time, we show here that cancer induction leads to a pronounced increase in heat sensitivity of peripheral nociceptors, which underlies cancer-induced heat hyperalgesia. Both changes are prevented by neutralization of TNFα. Although TNFα has been the focus of previous studies on cancer-related pain, we for the first time present direct links between TNFα, TRPV1 regulation, and an important role of TNFR2 in the development of heat hyperalgesia in cancer pain.

Although a number of candidate molecules have been associated with the generation of cancer pain, a mechanism-based understanding of tumor-induced heat hyperalgesia has not been available so far. Antagonizing the effects of bradykinin, endothelin, ATP, or certain neuropeptides in the bone cancer model had beneficial effects on pain-like behavior in humans or mouse (Davar G, 2001; Sevcik et al., 2005a,b). Neutralization of NGF improved bone cancer pain and reduced upregulation of ATF3 and other biochemical markers of nociceptor activation in the mouse (Sevcik et al., 2005a,b). Although nerve fibers have been found sprouting into the bone cancer tissue, little information on nociceptor function in cancer/metastasis has become available. In this model, the experimental approach to directly record from nociceptive afferents is very difficult and not applicable to investigating mechanisms of nociceptors at a larger scale. Therefore, we developed a soft tissue carcinoma model that allows us to delineate the mechanisms of the cancer-induced changes in nociceptive neurons related to heat hyperalgesia in a very well controlled preparation. We were able to obtain the first mechanistic electrophysiological data on cancer-related functional changes in nociceptors innervating cancer tissue. In bone cancer, 30% of the fibers were spontaneously active, and heat activation thresholds were decreased by 3.5°C (Cain et al., 2001a,b). We show similar changes of nociceptors *in vitro*, which were largely prevented after etanercept treatment, suggesting that endogenous TNFα upregulated nociceptor heat sensitivity at the tumor site. Histology of our experimental tumor shows dedifferentiated carcinoma cells at various mitotic stages and a pronounced infiltration of the neoplastic tissue with macrophages. This is similar to other models, in which cell types including malignant cells and immune cells (e.g., macrophages) were found (for review, see Mantyh et al., 2002). Macrophages are known as potential sources for proinflammatory and proalgesic cytokines such as TNFα (for review, see Mantyh, 2006). Converging evidence points to strong correlations between the number of macrophages, the level of TNFα production, and the development of heat hyperalgesia in inflam-

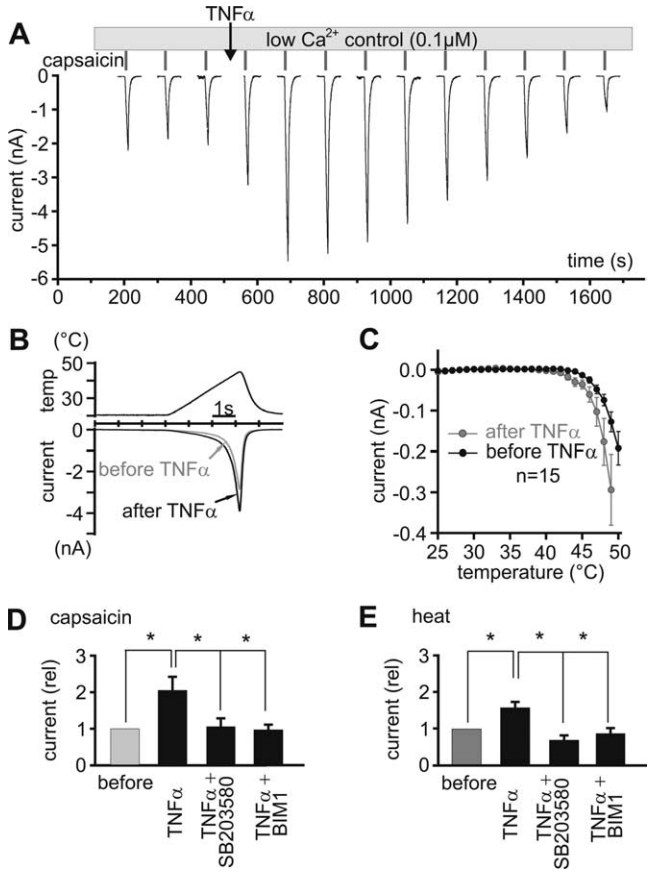

Figure 5. TNFα has a direct effect on TRPV1. ***A***, DRG neurons responded to capsaicin (0.5 μM) with a fast-activated inward current (I_{cap}), which was potentiated after a preconditioning stimulation with TNFα (1 ng/ml) for 60 s. ***B***, I_{heat} was elicited by identical 5 s ramp-shaped heat stimuli. ***C***, Pretreatment of DRG neurons with TNFα shifted the heat activation threshold to a lower temperature by 2°C ($n = 15$). ***D***, TNFα-induced potentiation of I_{cap} ($n = 13$; $p < 0.05$, Wilcoxon test) was abolished in the presence of the p38/MAP kinase inhibitor SB203580 (1 μM) and the PKC inhibitor BIM1 (1 μM; $n = 11$). ***E***, Stimulation of DRG neurons with TNFα (1 ng/ml) for 60 s induced sensitization of I_{heat} ($n = 21$; $p < 0.05$, Wilcoxon test), which was completely abolished in the presence of p38/MAP kinase inhibitor SB203580 (1 μM; $n = 8$) and PKC inhibitor BIM1 (1 μM; $n = 11$). ***D***, ***E***, Responses were normalized to the current amplitude immediately before TNFα application. Asterisks mark significant differences ($p < 0.05$, Wilcoxon test). rel, Relative; temp, temperature.

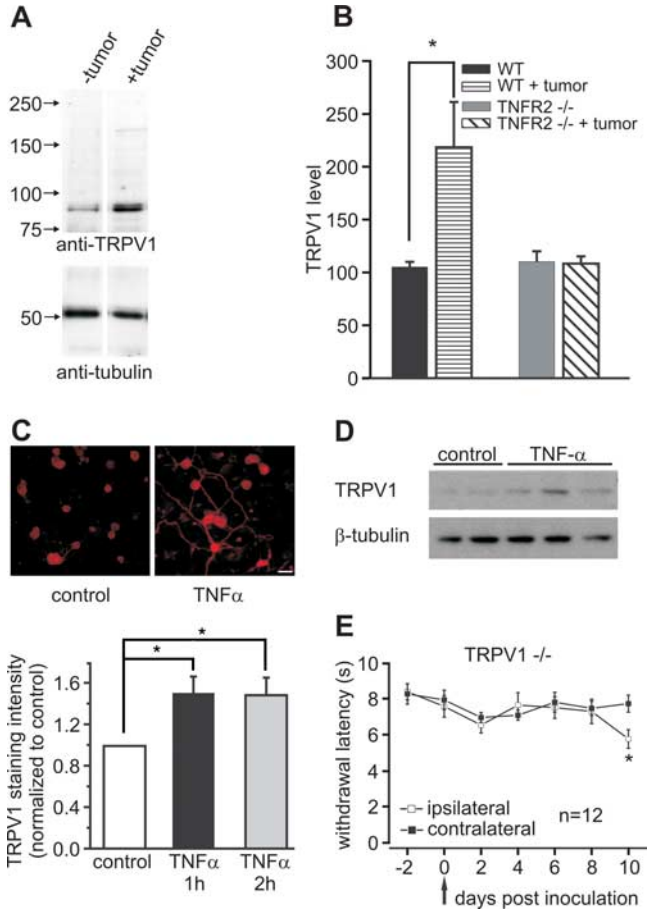

Figure 6. Heat hyperalgesia in the mice with tumor depended on TRPV1. ***A***, Western blot analysis of TRPV1 expression in L3, L4, and L5 DRG neurons from control and tumor mice. TRPV1 protein level is 2.1-fold increased in tumor compared with naive mice. ***B***, TRPV1 levels are significantly increased in tumor-bearing wild-type ($n = 6$) but not TNFR2 $^{-/-}$ ($n = 3$) mice. ***C***, Immunocytochemistry illustrates an increase in TRPV1 levels after TNFα (10 ng/ml) stimulation of DRG neurons in culture. Scale bar, 50 μm. The intensity of TRPV1 labeling increased significantly 1 and 2 h after TNFα (10 ng/ml) stimulation ($p < 0.05$ compared with control, ANOVA). ***D***, TRPV1 protein level as detected by Western blot analysis was upregulated after TNFα (10 ng/ml) stimulation. ***E***, Mice lacking the TRPV1 gene developed heat hyperalgesia only on day 10 after tumor induction ($n = 12$). Asterisks mark significant differences ($p < 0.05$, ANOVA). WT, Wild type.

matory and neuropathic animal models (Sommer and Schafers, 1998; Inglis et al., 2005). Moreover, an alleviation of heat hyperalgesia was correlated with delayed recruitment of nonresident macrophages and reduced levels of TNFα expression in neuropathic mice (Sommer and Schafers, 1998). In clinical trials, anti-TNFα therapy in patients with rheumatoid arthritis prevented ongoing joint destruction and alleviated arthritic pain (Baumgartner et al., 2004; Moreland et al., 2006). Moreover, in two clinical studies anti-TNFα therapy was successfully used for treatment of refractory pain resulting from bone metastasis and chronic back pain. In both studies, a beneficial effect on pain scores was reported (Tobinick, 2003; Tobinick and Davoodifar, 2004). In our soft tissue carcinoma model, etanercept treatment alleviated heat hyperalgesia in the tumor mice when started at the day of tumor induction. The same treatment prevented sensitization of heat nociceptors projecting into the tumor area, suggesting that patients not only with arthritic but also with cancer pain could benefit from neutralizing TNFα therapy. However, etanercept did not reverse tumor-induce heat hypersensitivity when the treatment was started after heat hyperalgesia had already developed. This finding is in line with the role of TNFα in initiating the proinflammatory cytokine cascade.

TNFα is a pleiotropic cytokine that stimulates the production and release of other proalgesic factors from tumor or immune cells, which in turn could act on sensory neurons (Woolf et al., 1997). Although indirect effects of TNFα cannot be excluded, our data favor a direct effect on heat nociceptors, because TNFα induced heat hyperalgesia with short latency and a sensitization of nociceptors to heat *in vitro* when applied on the receptive field (Sorkin et al., 1997; Pollock et al., 2002; Schafers et al., 2003). In normal skin, the sensation of heat pain occurs at a temperature of ~ 44°C. This correlates well with the activation threshold temperature of polymodal nociceptors and of the nociceptor-specific heat transducer TRPV1 (Caterina et al., 1997; Tominaga et al., 1998), a member of the thermoTRP family of ion channels (Jordt et al., 2003). The sensitivity of TRPV1 to heat and capsaicin depends on the phosphorylation status of the channel at intracellular serine/threonine or tyrosine sites (Bhave et al., 2002; Rathee et al., 2002; Mandadi et al., 2006). Here, TNFα induced a fast increase both in capsaicin- and heat-activated current amplitudes

and a drop of the activation threshold by 2°C, which required p38/MAP kinase and PKC. TNFα activates intracellular pathways involving protein kinases including p38/MAPK and PKC (Vandenabeele et al., 1995). PKC phosphorylates TRPV1 at specific sites and affects channel function (Tominaga et al., 1998; Bhave et al., 2002). Some of the phosphorylation sites at intracellular domains of the TRPV1 channel protein do not show preference for PKC, PKA (protein kinase A), or CaMKII (calcium/calmodulin-dependent protein kinase II) and could be possible targets for p38 MAP kinase phosphorylation. The fast changes in heat and capsaicin sensitivity of the sensory neurons within 1 min of TNFα stimulation are likely attributable to posttranslational modification via phosphorylation of the already existing TRPV1 channels in the cell membrane and might play a role in the early initiation phase of heat hyperalgesia in tumor mice.

In addition to regulating TRPV1 channel function on the cell membrane, TNFα also has been reported to induce upregulation of TRPV1 expression within several hours (Nicol et al., 1997). We found that TRPV1 protein but not mRNA was also upregulated in DRG neurons innervating the tumor area in wild-type but not TNFR-null mutant mice. Conventional gene expression via transcriptional regulation often takes hours, starting from mRNA synthesis. However, translational regulation is much faster, starting from existing mRNAs. TRPV1 is a very unique molecule and tightly controlled by translational regulation. Ji et al. (2002) have shown that after complete Freund's adjuvant-induced inflammation, there is a robust increase of TRPV1 protein levels but not TRPV1 mRNA levels in the DRG, suggesting a translational regulation. We have used immunocytochemistry and Western blotting, two conventional techniques for demonstrating protein expression, to examine TRPV1 expression. Both methods have consistently shown an increase in TRPV1 levels in DRG neurons (Fig. 6*D*,*E*). This increase in TRPV1 protein levels in DRG neurons from tumor mice might contribute to maintaining tumor-induced heat hyperalgesia. Because the proalgesic effect of TNFα in our model seems to target a dual regulation of TRPV1, we performed control experiments on TRPV1$^{-/-}$ mice, which did not show signs of tumor-induced heat hyperalgesia as expected.

Both, TNFα-induced TRPV1 sensitization and upregulation of TRPV1 suggest that TNFα plays an important role in development of heat hyperalgesia in mice with tumor. TNFα binds to two different membrane receptors, TNFR1 and TNFR2 (for review, see Sommer and Kress, 2004). The expression of TNF receptors on sensory neurons is still controversially discussed (Sommer et al., 1998; Pollock et al., 2002; Li et al., 2004). Our behavioral data show that in TNFR1$^{-/-}$ mice, the development of heat hyperalgesia is delayed in the early phase but remains in the later phase of tumor progression. It therefore appears that TNFR1 is important for the early phase of heat hyperalgesia, whereas TNFR2 seems to be required for the induction of persistent hyperalgesia. In our soft tissue tumor/metastasis model, a considerable improvement of heat hyperalgesia was detected in TNFR2$^{-/-}$ mice. Moreover, in TNFR2$^{-/-}$ mice, the expression of TRPV1 channel protein in DRGs projecting in the tumor area was low and comparable with that from naive (healthy) mice. This implies that cancer-related heat hyperalgesia and TRPV1 upregulation to a large extend depended on TNFR2. TNFα is well known to affect tumor cell survival, cell attachment, and tumor vascularization (Marchand et al., 2005). In our model, the sizes of the experimental tumors were similar in wild-type and TNF receptor knock-out mice and also after etanercept treatment. This suggests that the beneficial effect observed in the present study was not attributable to antiproliferative effects of TNF neutralization. Paw diameters were reduced in TNFR1$^{-/-}$ but not in TNFR2$^{-/-}$ mice, which may indicate that the TNFR1 may contribute to tumor-induced inflammation and paw swelling. Inflammation-induced hyperalgesia was accompanied by an upregulation of TNFR1 mRNA in neurons (Li et al., 2004), and TNFR1 was predominantly involved in the generation of neuropathic pain (Sommer et al., 1998).

We conclude that TNFα that is synthesized and released in tumor tissue induces heat hyperalgesia by directly sensitizing nociceptive neurons innervating the tumor area. As the main target of TNFα signaling pathways, we identify TRPV1, which is upregulated in tumor-bearing mice. TNFα also causes fast sensitization of capsaicin and heat-activated ionic currents via p38/MAP kinase and PKC in DRG neurons. Endogenous TNFα requires TNFR2 to generate nociceptor sensitization and heat hyperalgesia in our mouse soft tissue cancer pain model. Together, our data support the use of TRPV1 and TNFα antagonists in the treatment of cancer pain. In particular, blockade of TNFR2 may open new avenues for pain management in cancer patients.

References

Alexander RB, Ponniah S, Hasday J, Hebel JR (1998) Elevated levels of proinflammatory cytokines in the semen of patients with chronic prostatitis/chronic pelvic pain syndrome. Urology 52:744–749.

Baumgartner SW, Fleischmann RM, Moreland LW, Schiff MH, Markenson J, Whitmore JB (2004) Etanercept (Enbrel) in patients with rheumatoid arthritis with recent onset versus established disease: improvement in disability. J Rheumatol 31:1532–1537.

Bhave G, Zhu W, Wang H, Brasier DJ, Oxford GS, Gereau RW (2002) cAMP-dependent protein kinase regulates desensitization of the capsaicin receptor (VR1) by direct phosphorylation. Neuron 35:721–731.

Blumer MJ, Gahleitner P, Narzt T, Handl C, Ruthensteiner B (2002) Ribbons of semithin sections: an advanced method with a new type of diamond knife. J Neurosci Methods 120:11–16.

Cain DM, Wacnik PW, Simone DA (2001a) Animal models of cancer pain may reveal novel approaches to palliative care. Pain 91:1–4.

Cain DM, Wacnik PW, Turner M, Wendelschafer-Crabb G, Kennedy WR, Wilcox GL, Simone DA (2001b) Functional interactions between tumor and peripheral nerve: changes in excitability and morphology of primary afferent fibers in a murine model of cancer pain. J Neurosci 21:9367–9376.

Caterina MJ, Schumacher MA, Tominaga M, Rosen TA, Levine JD, Julius D (1997) The capsaicin receptor: a heat-activated ion channel in the pain pathway. Nature 389:816–824.

Chuang HH, Prescott ED, Kong H, Shields S, Jordt SE, Basbaum AI, Chao MV, Julius D (2001) Bradykinin and nerve growth factor release the capsaicin receptor from PtdIns(4,5)P2-mediated inhibition. Nature 411:957–962.

Davar G (2001) Endothelin-1 and metastatic cancer pain. Pain Med 2:24–27.

Davis JB, Gray J, Gunthorpe MJ, Hatcher JP, Davey PT, Overend P, Harries MH, Latcham J, Clapham C, Atkinson K, Hughes SA, Rance K, Grau E, Harper AJ, Pugh PL, Rogers DC, Bingham S, Randall A, Sheardown SA (2000) Vanilloid receptor-1 is essential for inflammatory thermal hyperalgesia. Nature 405:183–187.

Dittert I, Vlachova V, Knotkova H, Vitaskova Z, Vyklicky L, Kress M, Reeh PW (1998) A technique for fast application of heated solutions of different composition to cultured neurones. J Neurosci Methods 82:195–201.

Erickson SL, de Sauvage FJ, Kikly K, Carver-Moore K, Pitts-Meek S, Gillett N, Sheehan KC, Schreiber RD, Goeddel DV, Moore MW (1994) Decreased sensitivity to tumour-necrosis factor but normal T-cell development in TNF receptor-2-deficient mice. Nature 372:560–563.

Forster C, Handwerker HO (1990) Automatic classification and analysis of microneurographic spike data using a PC/AT. J Neurosci Methods 31:109–118.

Ghilardi JR, Rohrich H, Lindsay TH, Sevcik MA, Schwei MJ, Kubota K, Halvorson KG, Poblete J, Chaplan SR, Dubin AE, Carruthers NI, Swanson D, Kuskowski M, Flores CM, Julius D, Mantyh PW (2005) Selective blockade of the capsaicin receptor TRPV1 attenuates bone cancer pain. J Neurosci 25:3126–3131.

Hargreaves K, Dubner R, Brown F, Flores C, Joris J (1988) A new and sensitive method for measuring thermal nociception in cutaneous hyperalgesia. Pain 32:77–88.

Honore P, Schwei J, Rogers SD, Salak-Johnson JL, Finke MP, Ramnaraine ML, Clohisy DR, Mantyh PW (2000) Cellular and neurochemical remodeling of the spinal cord in bone cancer pain. Prog Brain Res 129:389–397.

Inglis JJ, Nissim A, Lees DM, Hunt SP, Chernajovsky Y, Kidd BL (2005) The differential contribution of tumour necrosis factor to thermal and mechanical hyperalgesia during chronic inflammation. Arthritis Res Ther 7:R807–R816.

Ji RR, Samad TA, Jin SX, Schmoll R, Woolf CJ (2002) p38 MAPK activation by NGF in primary sensory neurons after inflammation increases TRPV1 levels and maintains heat hyperalgesia. Neuron 36:57–68.

Jordt SE, McKemy DD, Julius D (2003) Lessons from peppers and peppermint: the molecular logic of thermosensation. Curr Opin Neurobiol 13:487–492.

Junger H, Sorkin LS (2000) Nociceptive and inflammatory effects of subcutaneous TNFalpha. Pain 85:145–151.

Koltzenburg M, Stucky CL, Lewin GR (1997) Receptive properties of mouse sensory neurons innervating hairy skin. J Neurophysiol 78:1841–1850.

Kress M, Koltzenburg M, Reeh PW, Handwerker HO (1992) Responsiveness and functional attributes of electrically localized terminals of cutaneous C-fibers in vivo and in vitro. J Neurophysiol 68:581–595.

Li Y, Ji A, Weihe E, Schafer MK (2004) Cell-specific expression and lipopolysaccharide-induced regulation of tumor necrosis factor α (TNFα) and TNF receptors in rat dorsal root ganglion. J Neurosci 24:9623–9631.

Mandadi S, Tominaga T, Numazaki M, Murayama N, Saito N, Armati PJ, Roufogalis BD, Tominaga M (2006) Increased sensitivity of desensitized TRPV1 by PMA occurs through PKCepsilon-mediated phosphorylation at S800. Pain 123:106–116.

Mantyh PW (2006) Cancer pain and its impact on diagnosis, survival and quality of life. Nat Rev Neurosci 7:797–809.

Mantyh PW, Clohisy DR, Koltzenburg M, Hunt SP (2002) Molecular mechanisms of cancer pain. Nat Rev Cancer 2:201–209.

Marchand F, Perretti M, McMahon SB (2005) Role of the immune system in chronic pain. Nat Rev Neurosci 6:521–532.

Moreland LW, Weinblatt ME, Keystone EC, Kremer JM, Martin RW, Schiff MH, Whitmore JB, White BW (2006) Etanercept treatment in adults with established rheumatoid arthritis: 7 years of clinical experience. J Rheumatol 33:854–861.

Nicol GD, Lopshire JC, Pafford CM (1997) Tumor necrosis factor enhances the capsaicin sensitivity of rat sensory neurons. J Neurosci 17:975–982.

Niiyama Y, Kawamata T, Yamamoto J, Omote K, Namiki A (2007) Bone cancer increases transient receptor potential vanilloid subfamily 1 expression within distinct subpopulations of dorsal root ganglion neurons. Neuroscience.

Obreja O, Rathee PK, Lips KS, Distler C, Kress M (2002) IL-1 beta potentiates heat-activated currents in rat sensory neurons: involvement of IL-1RI, tyrosine kinase, and protein kinase C. FASEB J 16:1497–1503.

Obreja O, Biasio W, Andratsch M, Lips KS, Rathee PK, Ludwig A, Rose-John S, Kress M (2005) Fast modulation of heat-activated ionic current by proinflammatory interleukin 6 in rat sensory neurons. Brain 128:1634–1641.

Pollock J, McFarlane SM, Connell MC, Zehavi U, Vandenabeele P, MacEwan DJ, Scott RH (2002) TNF-alpha receptors simultaneously activate Ca2+ mobilisation and stress kinases in cultured sensory neurones. Neuropharmacology 42:93–106.

Rathee PK, Distler C, Obreja O, Neuhuber W, Wang GK, Wang SY, Nau C, Kress M (2002) PKA/AKAP/VR-1 module: A common link of Gs-mediated signaling to thermal hyperalgesia. J Neurosci 22:4740–4745.

Rothe J, Lesslauer W, Lotscher H, Lang Y, Koebel P, Kontgen F, Althage A, Zinkernagel R, Steinmetz M, Bluethmann H (1993) Mice lacking the tumour necrosis factor receptor 1 are resistant to TNF-mediated toxicity but highly susceptible to infection by *Listeria* monocytogenes. Nature 364:798–802.

Sasamura T, Nakamura S, Iida Y, Fujii H, Murata J, Saiki I, Nojima H, Kuraishi Y (2002) Morphine analgesia suppresses tumor growth and metastasis in a mouse model of cancer pain produced by orthotopic tumor inoculation. Eur J Pharmacol 441:185–191.

Schafers M, Sorkin LS, Geis C, Shubayev VI (2003) Spinal nerve ligation induces transient upregulation of tumor necrosis factor receptors 1 and 2 in injured and adjacent uninjured dorsal root ganglia in the rat. Neurosci Lett 347:179–182.

Schwei MJ, Honore P, Rogers SD, Salak-Johnson JL, Finke MP, Ramnaraine ML, Clohisy DR, Mantyh PW (1999) Neurochemical and cellular reorganization of the spinal cord in a murine model of bone cancer pain. J Neurosci 19:10886–10897.

Sevcik MA, Ghilardi JR, Peters CM, Lindsay TH, Halvorson KG, Jonas BM, Kubota K, Kuskowski MA, Boustany L, Shelton DL, Mantyh PW (2005a) Anti-NGF therapy profoundly reduces bone cancer pain and the accompanying increase in markers of peripheral and central sensitization. Pain 115:128–141.

Sevcik MA, Ghilardi JR, Halvorson KG, Lindsay TH, Kubota K, Mantyh PW (2005b) Analgesic efficacy of bradykinin B1 antagonists in a murine bone cancer pain model. J Pain 6:771–775.

Shimoyama M, Tanaka K, Hasue F, Shimoyama N (2002) A mouse model of neuropathic cancer pain. Pain 99:167–174.

Sommer C, Kress M (2004) Recent findings on how proinflammatory cytokines cause pain: peripheral mechanisms in inflammatory and neuropathic hyperalgesia. Neurosci Lett 361:184–187.

Sommer C, Schafers M (1998) Painful mononeuropathy in C57BL/Wld mice with delayed wallerian degeneration: differential effects of cytokine production and nerve regeneration on thermal and mechanical hypersensitivity. Brain Res 784:154–162.

Sorkin LS, Xiao WH, Wagner R, Myers RR (1997) Tumour necrosis factor-alpha induces ectopic activity in nociceptive primary afferent fibres. Neuroscience 81:255–262.

Tobinick E, Davoodifar S (2004) Efficacy of etanercept delivered by perispinal administration for chronic back and/or neck disc-related pain: a study of clinical observations in 143 patients. Curr Med Res Opin 20:1075–1085.

Tobinick EL (2003) Targeted etanercept for treatment-refractory pain due to bone metastasis: two case reports. Clin Ther 25:2279–2288.

Tominaga M, Caterina MJ, Malmberg AB, Rosen TA, Gilbert H, Skinner K, Raumann BE, Basbaum AI, Julius D (1998) The cloned capsaicin receptor integrates multiple pain-producing stimuli. Neuron 21:531–543.

Vandenabeele P, Declercq W, Beyaert R, Fiers W (1995) Two tumour necrosis factor receptors: structure and function. Trends Cell Biol 5:392–399.

Wacnik PW, Eikmeier LJ, Ruggles TR, Ramnaraine ML, Walcheck BK, Beitz AJ, Wilcox GL (2001) Functional interactions between tumor and peripheral nerve: morphology, algogen identification, and behavioral characterization of a new murine model of cancer pain. J Neurosci 21:9355–9366.

Wacnik PW, Eikmeier LJ, Simone DA, Wilcox GL, Beitz AJ (2005) Nociceptive characteristics of tumor necrosis factor-alpha in naive and tumor-bearing mice. Neuroscience 132:479–491.

Woolf CJ, Allchorne A, Safieh-Garabedian B, Poole S (1997) Cytokines, nerve growth factor and inflammatory hyperalgesia: the contribution of tumour necrosis factor alpha. Br J Pharmacol 121:417–424.